SOFT ROBOTICS
Volume 00, Number 00, 2024

DOI: 10.1089/soro.2023.0204

SoRo
Soft Robotics

A Fast Online Elastic-Spine-Based Stiffness Adjusting Mechanism for Fishlike Swimming

Xiaocun Liao,[1,2] Chao Zhou,[1] Long Cheng,[2,3] Jian Wang,[1] Junfeng Fan,[1] and Zhuoliang Zhang[1]

Abstract

Fish tunes fishtail stiffness by coordinating its tendons, muscles, and other tissues to improve swimming performance. For robotic fish, achieving a fast and online fishlike stiffness adjustment over a large-scale range is of great significance for performance improvement. This article proposes an elastic-spine-based variable stiffness robotic fish, which adopts spring steel to emulate the fish spine, and its stiffness is adjusted by tuning the effective length of the elastic spine. The stiffness can be switched in the maximum adjustable range within 0.26 s. To optimize the motion performance of robotic fish by adjusting fishtail stiffness, a Kane-based dynamic model is proposed, based on which the stiffness adjustment strategy for multistage swimming is constructed. Simulations and experiments are conducted, including performance measurements and analyses in terms of swimming speed, thrust, and so on, and online stiffness adjustment-based multistage swimming, which verifies the feasibility of the proposed variable stiffness robotic fish. The maximum speed and lowest cost of transport for robotic fish are 0.43 m/s (equivalent to 0.81 BL/s) and 7.14 J/(kg·m), respectively.

Keywords: robotic fish, elastic spine, variable stiffness, stiffness adjustment strategy

Introduction

Owing to long-term evolution and natural selection, fish features remarkable swimming performances, for example, good maneuverability and high efficiency, which arouses researchers' interest.[1] Inspired by natural fish, many efforts have focused on bionic robotic fish, which achieve underwater propulsion by imitating fish's swimming. Recently, a variety of robotic fishes that are based on discrete joints,[2,3] smart material,[4] fluid-driven actuator,[5–7] wire-driven mode,[8] magnetic actuated system,[9,10] tensegrity joints,[11] and so on have been developed successfully.

It is reported that passive flexible fishtail can adapt to water flow well, and produce elastic deformation by interacting with fluid, which results in periodic energy-storing, thus improving propulsive performance.[12–16] How to adjust the stiffness of flexible fishtail is challenging. There are two ways of adjusting stiffness, including offline[15–18] and online[19–26] variable stiffness.

The most common method to achieve offline variable stiffness is replacing different components, such as elastic components with different stiffness. Chen et al. developed a miniature robotic fish with passive flexible joint based on dual torsion springs, and the stiffness of torsion spring was tuned offline, thus improving swimming performance.[15] Behbahani

[1]Laboratory of Cognition and Decision Intelligence for Complex Systems, Institute of Automation, Chinese Academy of Sciences, Beijing, China.
[2]School of Artificial Intelligence, University of Chinese Academy of Sciences, Beijing, China.
[3]State Key Laboratory of Multimodal Artificial Intelligence Systems, Institute of Automation, Chinese Academy of Sciences, Beijing, China.

et al. offline tuned the stiffness and length of flexible passive rowing joint to improve the propulsion performance and efficiency of robotic fish.[16] A robotic fish with offline variable stiffness decoupled mechanism was proposed by Li et al., and stiffness adjustment was realized by replacing the springs with different stiffness to achieve pretension adjustment.[17]

For offline variable stiffness, robotic fish cannot achieve stiffness adjustment during swimming process. It is impossible for these robotic fishes to realize real-time optimal performance by adjusting stiffness online according to real-time swimming state. Hence, online variable stiffness becomes a better choice for real-time performance improvement.

For online variable stiffness, robotic fish can adjust stiffness at any time to enhance swimming performance especially when swimming. This inspiration is taken from natural fish. Some researchers have shown that fish can tune stiffness dynamically by coordinating muscles, tendons, and other tissues during swimming, to adapt to the survival needs in different scenarios.[27–30] For example, fish can dynamically adjust fishtail stiffness to adapt to sudden water flow for maintaining high swimming performance. The stiffness adjustment allows fish to display capabilities during preying and escape.

As for online variable stiffness, there are various variable stiffness mechanisms, which are mainly based on smart materials,[19,20] fluid base soft actuator,[21,22] traditional mechanism,[23–26] and so on.

Some smart materials, for example, shape memory alloy (SMA), and electrorheological (ER) fluids, whose physical or chemical characteristics are changed by external stimulus, such as electric field, magnetic field, or temperature, can be adopted to adjust fishtail stiffness. Behbahani and Tan designed a variable stiffness fish fin based on ER fluid.[19] The stiffness was tuned fleetly by changing electric field. Preliminary results were obtained on variable stiffness fish fin instead of the untethered robotic fish. Besides, high voltage was required to stimulate ER fluid, introducing high power loss. A tunable stiffness caudal peduncle developed by Liu et al. was made of SMA, whose stiffness was tuned by electric heating.[20] It was inefficient to heat SMA in water, resulting in that the response time of stiffness adjustment was relatively long, and energy loss was also high. Although heating SMA to increase stiffness was easy, heat dissipation to reduce stiffness was challenging and could only be achieved by thermal conduction with surrounding.

Moreover, tuning the fluid pressure of soft actuator to adjust stiffness is also an effective method. Jusufi et al. achieved the fishlike back-and-forth swing and stiffness adjustment by tuning the fluid pressure of two pneumatic actuators fixed on both sides of the flexible fishtail.[21] Profiting from the stiffness adjustment, high thrust was generated for the robotic fishtail. Ju and Yun adjusted the volume of water in the long cylindrical space inside fishtail to adjust stiffness, and their robotic fish obtained a maximum swimming speed of 0.64 BL/s.[22] Fast stiffness adjustment is also challenging for the fluid-based variable stiffness actuator since the response rate of fluid is limited, which introduces some novel challenges for real-time control. Also, the adjustable stiffness range is relatively small scale.

Traditional mechanisms, for example, changing fishtail shape parameters and spring pretension, can provide a more stable and reliable way to tune stiffness. Park et al. developed a fishtail, whose stiffness was adjusted by utilizing tendons to compress fishtail along with body axis.[23] The stiffness adjustment was also accompanied by the shape deformation of fishtail, which made robotic fish difficult to maintain a streamlined shape. Ziegler et al. developed a tethered four-joint robot in which the final three passive joints each had a pretensioned spring to tune stiffness.[24]

Similarly, Zhong et al. designed a variable stiffness robotic fish, and spring pretension was adjusted by servomotor to achieve stiffness adjustment.[25] For the method of changing spring pretension, the effect of fishtail against fluid is increased due to the increase in pretension force, thereby achieving the purpose of tuning stiffness. This method results in the dead band of fishtail swing, where the passive joint angle is 0° periodically when the effect of hydrodynamic forces is less than that of spring pretension.

Achieving a fast and online fishlike stiffness adjustment over a large-scale range is of great significance for the performance improvement and practical application of robotic fish. Since there is no one best stiffness that always enables optimal swimming performance for different motion states, using online adjustable stiffness becomes a logical method.[31] For example, based on real-time motion state, robotic fish can adjust fishtail stiffness to maintain optimal performance: the highest speed, the lowest power consumption.

Besides, adjusting stiffness and swing rhythm simultaneously is capable of maneuverability improvement to pursue high turning speed and small turning radius, thus enhancing robotic fish's ability to avoid obstacles quickly and turn fleetly, especially in narrow areas. To this end, this article proposes a mechanism with the ability to adjust stiffness fleetly over a large-scale range. Based on the proposed dynamic model, the propulsive performance of robotic fish under different stiffness is analyzed, and stable and efficient multistage swimming is achieved by online adjustable stiffness. The main contributions are concluded as follows:

1. A variable stiffness mechanism, which adjusts fishtail stiffness by tuning the effective length of elastic component, is presented. It is capable of fast and online adjusting stiffness over a large-scale range. The adjustable stiffness ranges from 17.62 to 184.7 N/m.
2. A Kane-based dynamic model of robotic fish is proposed to analyze the effect of stiffness variation on propulsive performance and to optimize propulsive performance. Results reveal that propulsive performance is closely related to fishtail stiffness, and the optimal stiffness that maximizes swimming speed and thrust holds a positive correlation with frequency.
3. To determine optimal stiffness for efficient multistage swimming so as to adapt to various application scenarios, a stiffness adjustment strategy with the purpose of minimizing power consumption and the error between the current and desired speed is constructed.

Design and Control of Variable Stiffness Robotic Fish

Mechatronics design

As shown in Figure 1a, fish have powerful muscles, complex spines, and strong tendons in posterior body, enabling their amazing underwater mobility. Many researchers show that fishtail stiffness can be tuned by coordinating tendons, muscles, and other tissues to improve swimming

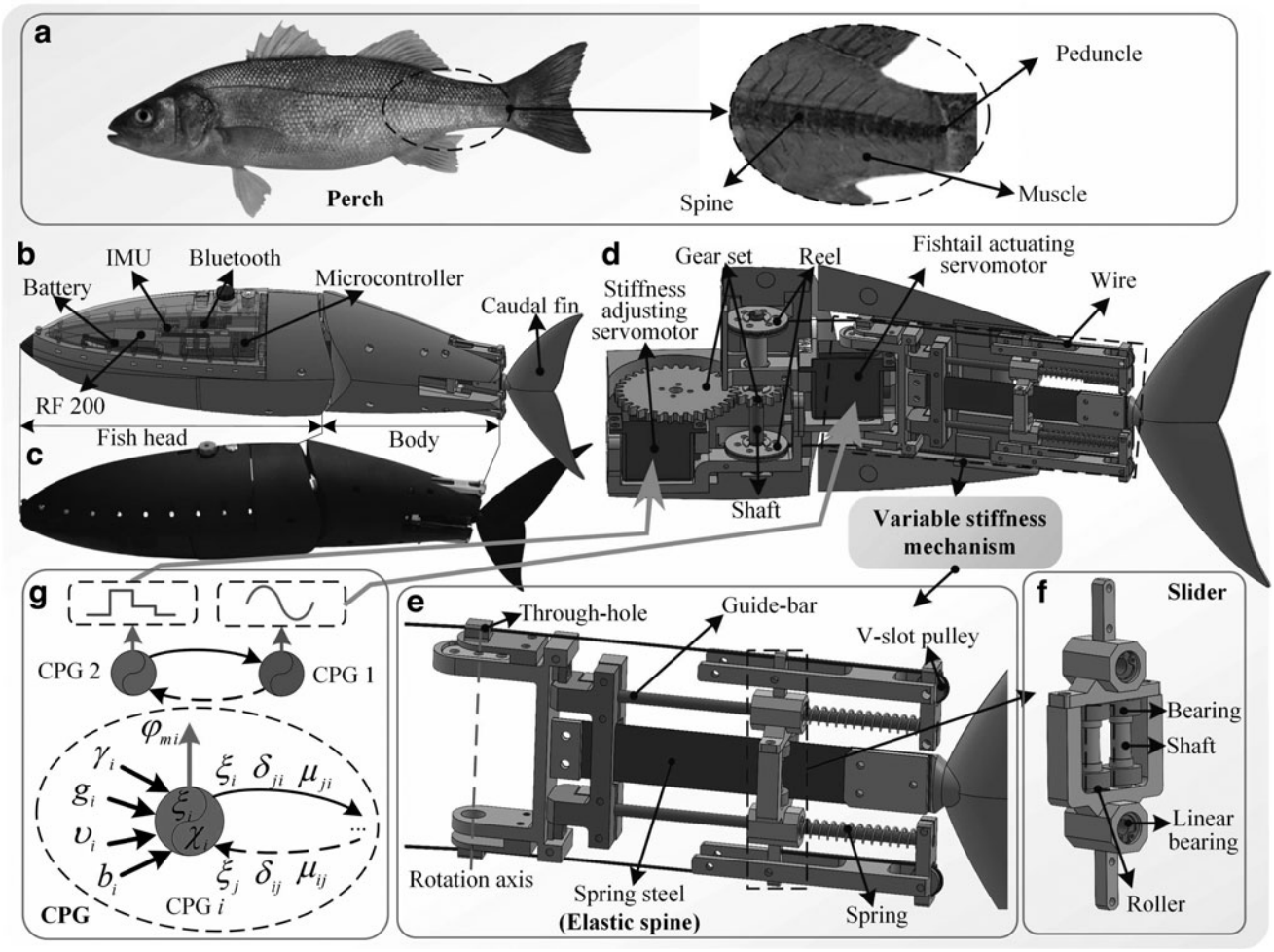

FIG. 1. Overview of the variable stiffness robotic fish. **(a)** *Left*: Perch. *Right*: The fishtail anatomy. **(b)** Schematic design. Fish head accommodates a microcontroller, battery, IMU, Bluetooth, and so on. **(c)** Robotic prototype. **(d)** Sectional view of the fishtail. The gear ratio of gear set and the reel's radius can be suitably adjusted according to the maximum adjustable length of spring steel. **(e)** Sketch of the variable stiffness mechanism. The spring steel is held by two rollers and the effective lengths of the fully constrained segment and the semiconstrained segment is determined by the position of the slider. **(f)** Sketch of the slider. Every roller includes two bearings and one shaft to reduce friction loss. To prevent the slider from being stuck, two linear bearings are mounted between the slider and guide-bar. More design specifics for the variable stiffness mechanism can be referred to Supplementary Appendix SA1. **(g)** Diagrammatic sketch of the central-pattern-generator-based control (see Supplementary Appendix SA2).

performance.[27–30] Some researchers believe that the stiffness variation of fishtail is induced by the changes in muscle activation. The co-contraction extent of the muscles on opposite sides of the body results in stiffness variation for fish.[31–33]

Particularly, fishtail features a convergent shape, that is, the closer the part of fishtail is to the caudal fin, the narrower its width is. This nonuniform cross-sectional areas of fishtail further enlarges the distribution complexity of fishtail stiffness. Taking inspiration from fish, the proposed variable stiffness robotic fish can tune fishtail stiffness fleetly over a large-scale range by adjusting the effective length of the spring-steel-based elastic spine. As shown in Figure 1, robotic fish consists of a fish head, fish body, driving mechanism, stiffness adjustment mechanism, and caudal fin.

Two servomotors, that is, fishtail actuating servomotor and stiffness adjusting servomotor, are applied to achieve fishlike reciprocating swing and tune fishtail stiffness, respectively. Stiffness adjusting servomotor is connected to reel by gear set, which enables the backward motion of slider by wire. Since the wire is incapable of providing thrust, two springs are adopted to enable the forward motion of slider. The load of fishtail actuating servomotor is reduced by mounting the stiffness adjusting servomotor on its front side. The specifications of robotic fish can be referred to Supplementary Appendix SA6.

Obviously, the slider divides spring steel into two segments. The anterior segment of spring steel is named the fully constrained segment, whose both ends are constrained. The rear segment of spring steel, whose one end is constrained by the slider and the other end is free completely, is referred to as the semiconstrained segment. When spring steel is not completely fixed to roller, both the fully constrained segment and semiconstrained segment bend due to the interaction between fishtail and fluid. The slider position determines the lengths of the two segments, thus determining fishtail stiffness.

Central-pattern-generator-based control

The central pattern generator (CPG) made up of several oscillators is capable of yielding rhythmic signals without any

feedback and is widely exploited in robotic fish. Given that two servomotors are adopted, a CPG network with two Ijspeert's oscillators[34] is constructed to control robotic fish, as shown in Figure 1g. The first oscillator outputs the periodic sinusoid-like signal φ_{m1} applied to fishtail actuating servomotor for fishlike swing. However, the rectangular wave signal φ_{m2} with different amplitudes generated from the second oscillator is required for stiffness adjusting servomotor to tune and maintain slider position for stiffness adjustment.

Stiffness Adjustment Analysis

The equivalent fishtail stiffness is defined as

$$\kappa = \frac{F_S}{\ell} = \frac{3E_T I_T}{(l_{T2}+l_{cf})^2 l_{T1} + 3l_{cf} l_{T2}^2 + 3l_{cf}^2 l_{T2} + l_{T2}^3}, \quad (1)$$

where F_S and ℓ denote the force and deflection of caudal fin centroid; I_T and E_T are the area moment of inertia and elastic modulus of spring steel, respectively; l_T, l_{T1}, and l_{T2} are the lengths of the whole spring steel, fully constrained segment, and semiconstrained segment, respectively; l_{cf} denotes the distance between the caudal fin centroid and the free end of the semiconstrained segment. Any stiffness within the adjustable range can be switched within 0.26 s (see Supplementary Appendix SA3).

According to Equation (1), when slider moves backward under the action of wire, the length of the fully constrained segment becomes long, whereas the length of the semiconstrained segment becomes short, thus resulting in an increase in stiffness. The opposite conclusion can be obtained when slider moves forward. From Figure 2 it is observed that there is a linear variation between l_{Ti} ($i=1$, 2) and φ_{m2}, whereas a drastic increase in stiffness occurs as φ_{m2} increases. The minimum and maximum stiffness are 17.62 and 184.7 N/m, respectively, resulting in a ratio of about 10.48.

Dynamic Modeling and Locomotion Optimization

The propulsive performance of robotic fish depends on fishtail stiffness and can be effectively improved by online adjusting stiffness. This section presents a Kane-based dynamic model, which becomes an effective tool for performance analysis and motion optimization. Based on dynamic model, a stiffness adjustment strategy for multistage swimming is established to guide robotic fish how to adjust stiffness optimally.

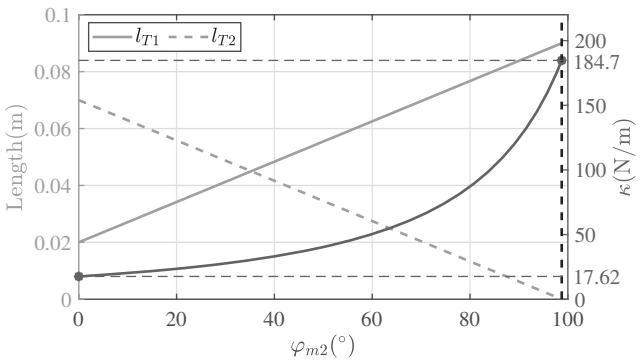

FIG. 2. The equivalent fishtail stiffness κ and the lengths of the fully constrained segment and semiconstrained segment versus φ_{m2}. The *black dotted line* stands for the maximum adjustable angle (about 98.75°) of stiffness adjusting servomotor.

Dynamic modeling

The dynamic model of robotic fish is expressed by the following equation (see Supplementary Appendix SA4):

$$\begin{cases} \boldsymbol{u} = \begin{bmatrix} \dot{x}_0 & \dot{y}_0 & \dot{\theta}_0 & \dot{\varphi}_1 & \dot{\varphi}_2 \end{bmatrix}^{\mathrm{T}} \\ \aleph_{5\times5}\dot{\boldsymbol{u}} = \Re_{5\times1} \end{cases}, \quad (2)$$

where $\aleph_{5\times5}$ and $\Re_{5\times1}$ denote the matrices of the equivalent mass and equivalent resultant force, respectively; $\boldsymbol{u}$ is the generalized velocity of robotic fish; x_0 and y_0 represent the position in axes X_w and Y_w of inertial reference frame for robotic fish, respectively; θ_0 denotes yaw angle; φ_1 is the active joint angle defined as the angle between fish head and body; φ_2 denotes the passive joint angle defined as the angle between fish body and caudal fin. The full states of robotic fish, including position, posture, and joint angle, can be obtained by solving dynamic model.

Stiffness adjustment strategy

The motion performance of robotic fish can be enhanced by adjusting stiffness in real time, which depends on an excellent stiffness adjustment strategy. How to achieve fine stiffness adjustment to obtain optimal performance is crucial. For some underwater missions, such as target tracking and cruising with constant speed, robotic fish are expected to swim at a steady speed, and another potential goal is to achieve low power consumption to enhance their endurance capability. Particularly, robotic fish need to respond to speed changes in multistage, where adjustable stiffness can play a significant role.

Hence, a multiobjective-optimization-based stiffness adjustment strategy for multistage swimming is proposed by using the proposed dynamic model. The purpose of this strategy is to optimize fishtail stiffness, frequency, and amplitude of each swimming stage so that robotic fish can maintain a stable speed and low power consumption simultaneously in multistage swimming. The optimization model is formulized by

$$\min_{\kappa_i,\ f_i,\ A_i} \begin{cases} \varepsilon_V = \sum_i \varepsilon_{V,i} \\ P_m = \sum_i P_{m,i} \end{cases}$$
$$s.t. \begin{cases} \boldsymbol{u} = \begin{bmatrix} \dot{x}_0 & \dot{y}_0 & \dot{\theta}_0 & \dot{\varphi}_1 & \dot{\varphi}_2 \end{bmatrix}^{\mathrm{T}} \\ \aleph_{5\times5}\dot{\boldsymbol{u}} = \Re_{5\times1} \\ \varepsilon_{V,i} = |V_i - V_{e,i}| \le \varepsilon_{Va} \\ \kappa^{min} \le \kappa_i \le \kappa^{max} \\ f^{min} \le f_i \le f^{max} \\ A^{min} \le A_i \le A^{max} \end{cases}, \quad (3)$$

where V_i and $V_{e,i}$ are the steady speed and expected speed for the ith swimming stage, respectively; $\varepsilon_{V,i}$ and $P_{m,i}$ denote the speed error and average power for the ith swimming stage, respectively; ε_V and P_m denote the speed error and average power for all swimming stages, respectively; ε_{Va} is the threshold of speed error; κ_i, f_i, and A_i denote the stiffness, frequency, and amplitude of fishtail swing on the ith swimming stage, respectively; κ^{min} and κ^{max} are the minimum and maximum stiffness, respectively. f^{min} and f^{max} represent the minimum and maximum frequency, respectively. A^{min} and A^{max} denote the minimum and maximum amplitude, respectively. The solution of Equation (3) can be referred to Supplementary Appendix SA5.

Experiments and Simulations

To verify the feasibility of mechatronics design and the developed models for robotic fish, extensive experiments and simulations are conducted.

Validation of fishtail stiffness model

To validate the proposed stiffness model, the deflections ℓ of the caudal fin centroid at different vertical forces F_S are obtained (see Supplementary Appendix SA8), as shown in Figure 3a. Obviously, greater forces are required to obtain the same deflection with stiffness increase, reflected by slope increase. Besides, simulations are in line with experiments, and all errors are within 5%, validating stiffness model.

Two sets of aquatic experiments are used to verify the effect of stiffness adjustment on fishlike swimming. Only stiffness is adjusted to focus on its effects on fishlike swimming. As shown in Figure 3c, when fishtail stiffness of 17.62 N/m is small, caudal fin lags behind fish body, and their angle is also large. The angle amplitude is about 53°. On the contrary, from Figure 3d, the angle between fish body and caudal fin is relatively small, and the angle amplitude is about 15°, when the stiffness of 184.7 N/m is large. For the designed variable stiffness robotic fish, stiffness can be adjusted to achieve large-scale adjustment of passive joint angle for high-performance fishlike swimming.

Thrust analysis

To explore swimming performance, thrust, the phase between active and passive joint angles, and the absolute angle of caudal fin are obtained (see Supplementary Appendix SA9). As depicted in Figure 4a, thrust first increases and then decreases for small stiffness as frequency increases. When stiffness is large, thrust features a positive correlation with frequency. From Figure 4b, it is found that phase difference always increases with the growth of frequency.

Comparing Figure 4a with b, it is obvious that phase difference corresponding to maximum thrust is $\sim 0.65\pi$ within the frequency range of 0–2 Hz. From Figure 4c, the absolute angle of caudal fin decreases as frequency increases for the given stiffness. When frequency is high and stiffness is small, the absolute angle of caudal fin is almost close to 0°, which is also the reason why the corresponding thrust is relatively small.

Analysis of swimming speed

Using the proposed dynamic model, the average swimming speeds at different combinations of stiffness and frequency are obtained (see Supplementary Appendix SA3 and SA7), as shown in Figure 5a. For small stiffness, speed first increases to a maximum and then decreases as frequency increases. When stiffness is large, there is a positive correlation between speed and frequency. The growth of frequency leads to an increase in optimal stiffness, which is reasonable since stiffness should be increased to respond to the increase of hydrodynamic forces for improving swimming speed.

From Figure 5b, compared with the variable stiffness, the maximum swimming speed can only be obtained at a certain frequency for the fixed stiffness. However, adjustable stiffness ensures that robotic fish maintains the optimal speed for

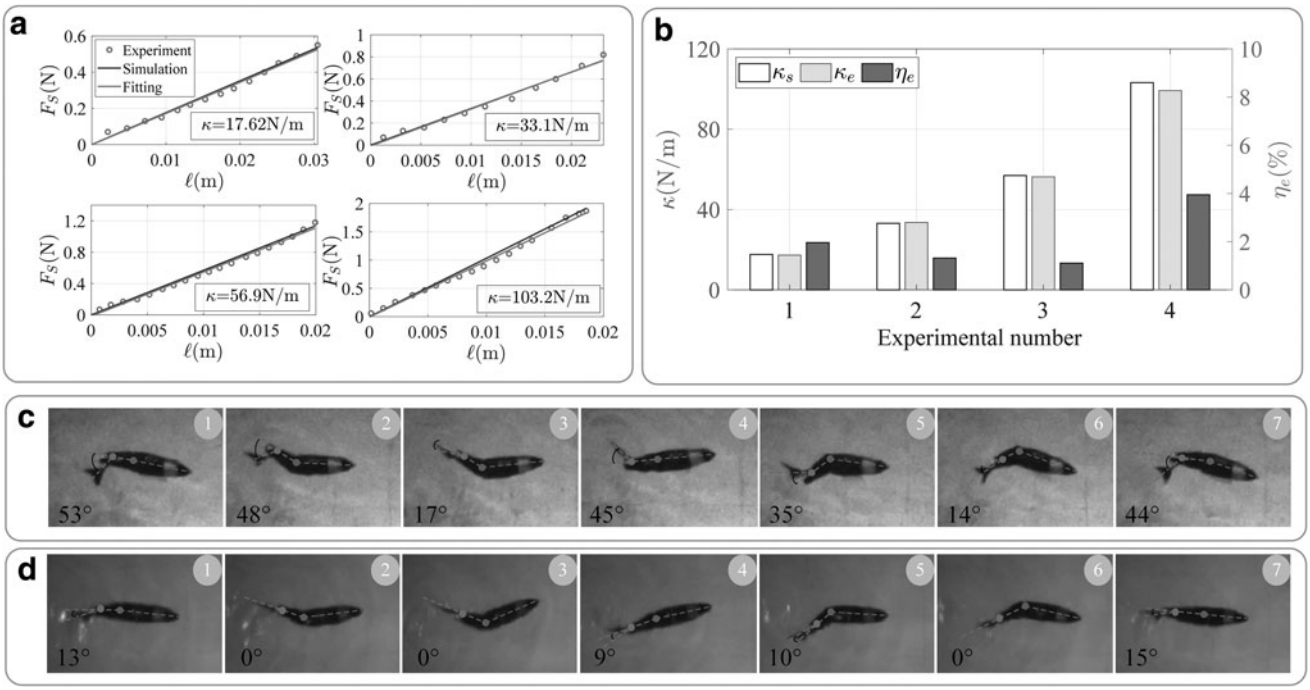

FIG. 3. **(a)** Experimental data and simulations of the deflection ℓ and force F_S for different fishtail stiffness. Based on the least square method, the experimental data are fitted by the linear fitting method, and the slope represents fishtail stiffness. **(b)** The fishtail stiffness comparison between simulation and experiment. The relative error is defined as $\eta_e = |\kappa_s - \kappa_e|/\kappa_e \times 100\%$, where κ_s and κ_e denote the simulation and experimental stiffness, respectively. **(c)** Free swimming of robotic fish (see Supplementary Movie S1). Fishtail stiffness, frequency, and amplitude are 17.62 N/m, 1 Hz, and 40°, respectively. The swimming speed is 0.20 m/s. **(d)** Free swimming of robotic fish (see Supplementary Movie S1). Fishtail stiffness, frequency, and amplitude are 184.7 N/m, 1 Hz, and 40°, respectively. The swimming speed is 0.25 m/s.

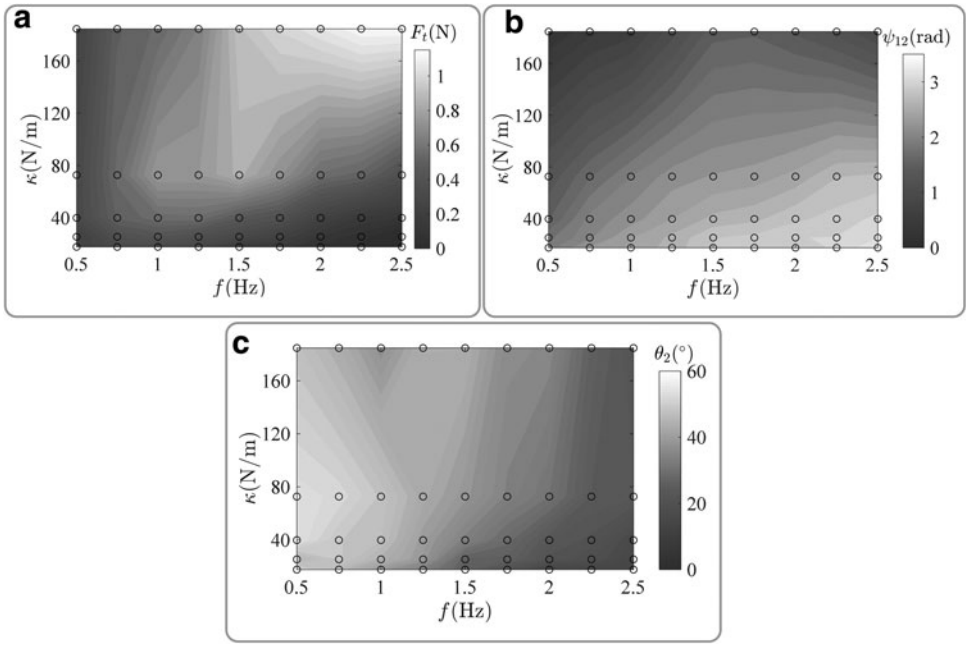

FIG. 4. **(a)** Fishtail thrust versus fishtail stiffness and frequency. **(b)** The phase ψ_{12} between active and passive joint angles versus fishtail stiffness and frequency. **(c)** The absolute angle θ_2 of caudal fin versus fishtail stiffness and frequency. In **(a–c)**, *circles* represent experimental data, and the swing amplitude of fishtail is 40°.

any frequency. By adjusting stiffness reasonably, the optimal speed features a linear relationship with frequency.

Figure 5c shows the experimental speeds at different combinations of stiffness and frequency (see Supplementary Appendix SA10). A conclusion similar to that of simulation can be drawn. That is, speed first increases and then decreases with the increase of frequency for small stiffness, and swimming speed is positively correlated with frequency for large stiffness. The changing trend of speed is similar to that of thrust, and the optimal stiffness determined by the maximum speed is the same as that of maximum thrust. There are acceptable errors between simulations and experiments, which are attributed to water wave disturbance, and so on. The maximum speed of 0.43 m/s (equivalent to 0.81 BL/s) is obtained when frequency and stiffness are 2.5 Hz and 184.7 N/m, respectively.

Swimming performance evaluation

Stride length (*SL*) can reflect swimming performance for robotic fish.[11] From Figure 6a, *SL* first increases and then

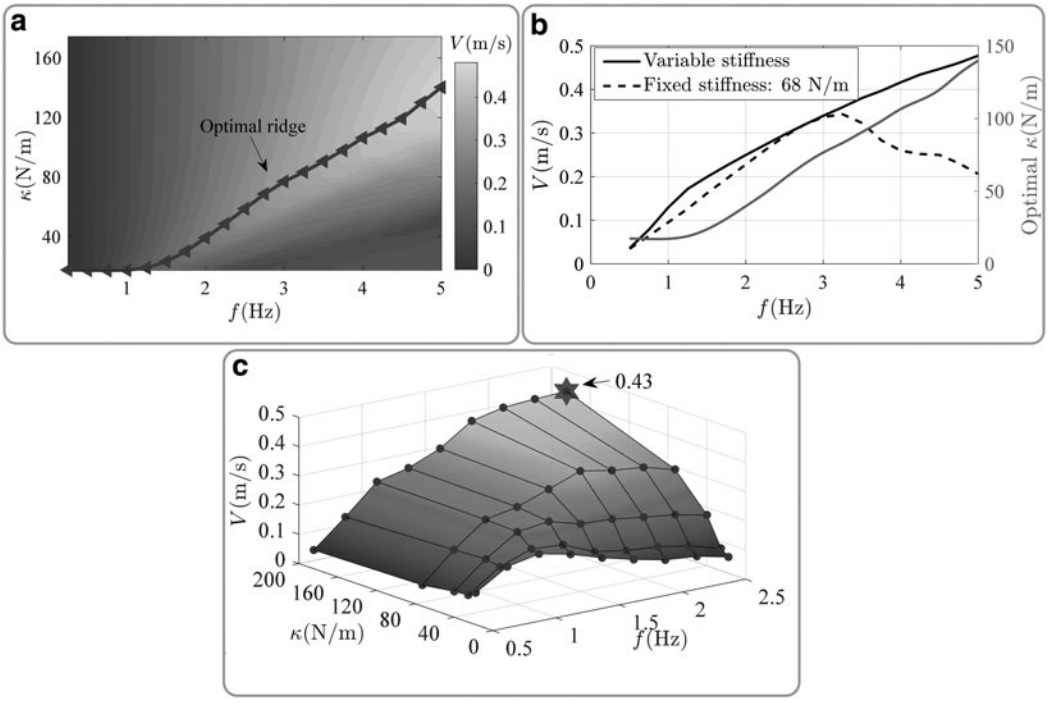

FIG. 5. Analysis of swimming speed. The swing amplitude of fishtail is 40°. **(a)** Simulation speed versus fishtail stiffness and frequency. **(b)** Optimal speed and stiffness versus frequency. **(c)** Experimental speed versus fishtail stiffness and frequency. *Points* represent experimental data.

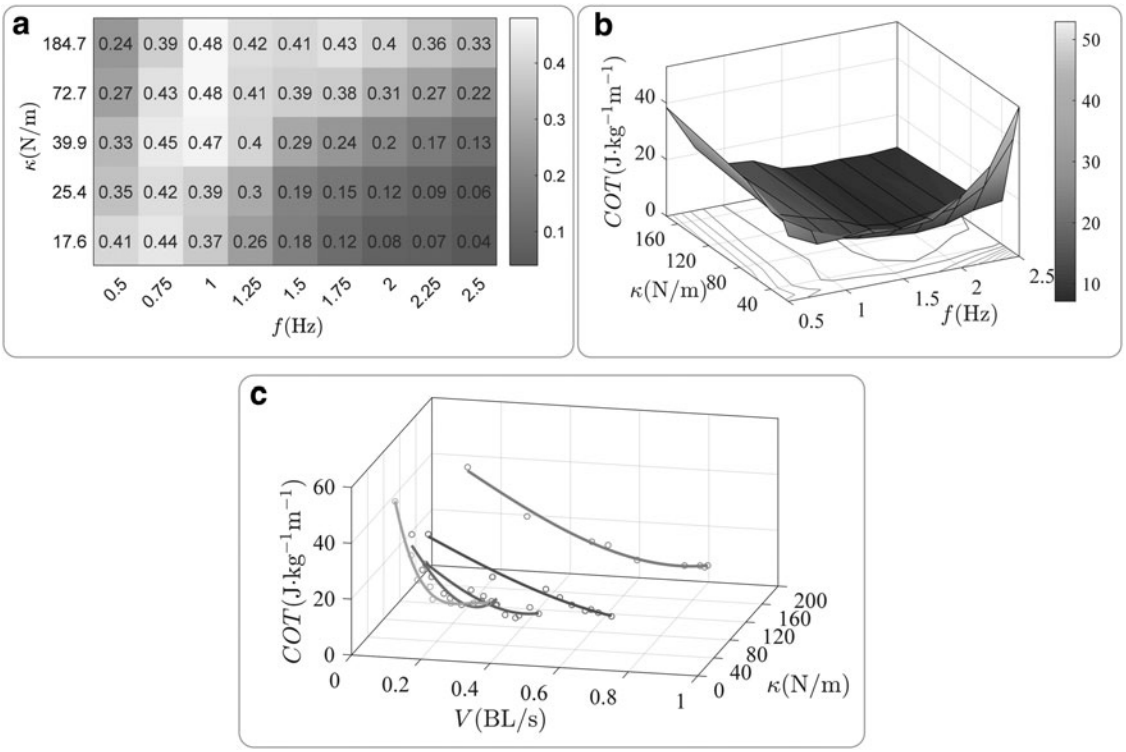

FIG. 6. Swimming performance evaluation of robotic fish. The swing amplitude of fishtail is 40°. **(a)** *SL* (BL/cycle) versus frequency and fishtail stiffness. SL (SL = *V*/*f*) represents the distance moved within a fishtail swing cycle, where *V* and *f* denote speed and frequency, respectively. **(b)** *COT* (J/[kg·m]) versus frequency and fishtail stiffness. *COT* is defined as the energy consumed to move an object of unit mass over a unit distance. That is, $COT = P_m/V/m$, where P_m and m denote the power consumption and mass of robotic fish, respectively. Grid intersections represent experimental data. **(c)** *COT* (J/[kg·m]) versus speed and fishtail stiffness.

decreases with the increase of frequency. For low frequencies (0.5–0.75 Hz), *SL* decreases overall as stiffness increases. When frequency is >0.75 Hz, *SL* increases as stiffness increases. Comparing Figure 5c with Figure 6a, it can be found that the stiffness corresponding to the optimal *SL* is consistent with that of the optimal speed. When frequency and stiffness are 1 Hz and 184.7 N/m, respectively, the maximum *SL* is 0.48 BL/cycle, which is close to that of biological fish (∼0.71 BL/cycle).[11]

Besides, the cost of transport (*COT*) demonstrated in Figure 6b and c is applied to assess swimming efficiency.[3] When stiffness is small, *COT* decreases first and then increases with the increase in frequency. When stiffness is large, *COT* features a decreasing trend as frequency increases. The lowest *COT* of 7.14 J/(kg·m) is obtained when stiffness and frequency are 72.7 N/m and 1.75 Hz, respectively. Besides, as swimming speed increases, *COT* first decreases and then increases slightly. When swimming speed is within the range of 0.2–0.3 BL/s, small stiffness enables low *COT*, thus resulting in high propulsion efficiency. When swimming speed is >0.4 BL/s, the greater the stiffness becomes, the lower the *COT* is, and the higher the propulsion efficiency is.

Stiffness adjustment experiment

Online stiffness adjustment enables real-time high-performance swimming for robotic fish. To verify the aforementioned stiffness adjustment strategy, simulations and experiments are conducted to verify the efficient three-stage swimming. The desired speeds for three-stage swimming are 0.1, 0.2, and 0.3 m/s, respectively.

According to the aforementioned optimization goal, a trade-off between ε_V and P_m needs to be made. Using the proposed optimization model, the distributions of ε_V and P_m, and the Pareto-optimal front are obtained, as shown in Figure 7a. The averages of ε_V and P_m for Pareto-optimal front, that is, $\bar{\varepsilon}_V$ and $\bar{P}_m$, are 0.045 m/s and 1.20 W, respectively. Furthermore, the point on the Pareto-optimal front, which holds a trade-off between ε_V and P_m, is selected, as shown by the diamond in Figure 7a.

The corresponding stiffness, frequencies, and amplitudes for the three stages are obtained and applied to swimming experiment for robotic fish. For three-stage swimming, simulation and experimental ε_V are 0.05 and 0.058 m/s, respectively. The difference between simulation and experimental ε_V is 0.008 m/s, which is attributed to the water wave disturbance, and so on. The deviation in P_m between simulation and experiment exists, which is attributed to the fact that the losses of servomotor and circuit are difficult to model accurately.

Obviously, the response time of performing two stiffness adjustment in Figure 8 are about 0.16 and 0.18 s, respectively, indicating that the designed variable stiffness mechanism features a fast response to stiffness adjustment. Since speed cannot be mutated abruptly, it takes more time for robotic fish to reach a stable state after tuning fishtail stiffness. The settling time of swimming is defined as the duration required to transition from a stable swimming state under one stiffness to

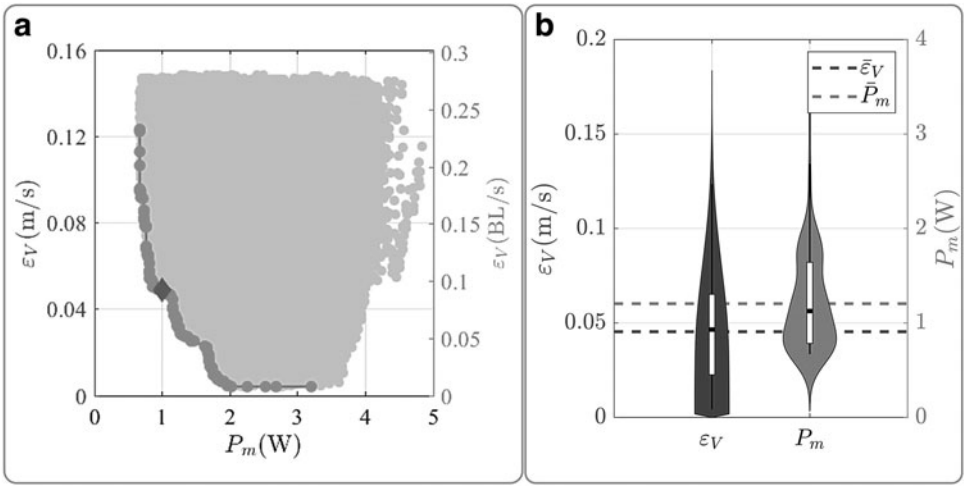

FIG. 7. Simulation of three-stage swimming. **(a)** The distributions of ε_V and P_m under all feasible solutions. The *dark color points* represent the Pareto-optimal front, each solution of which is not dominated by other solutions. The solutions on the Pareto-optimal front can guarantee that the speed error is small while keeping the power consumption as low as possible for robotic fish. **(b)** The distributions of ε_V and P_m for the Pareto-optimal front.

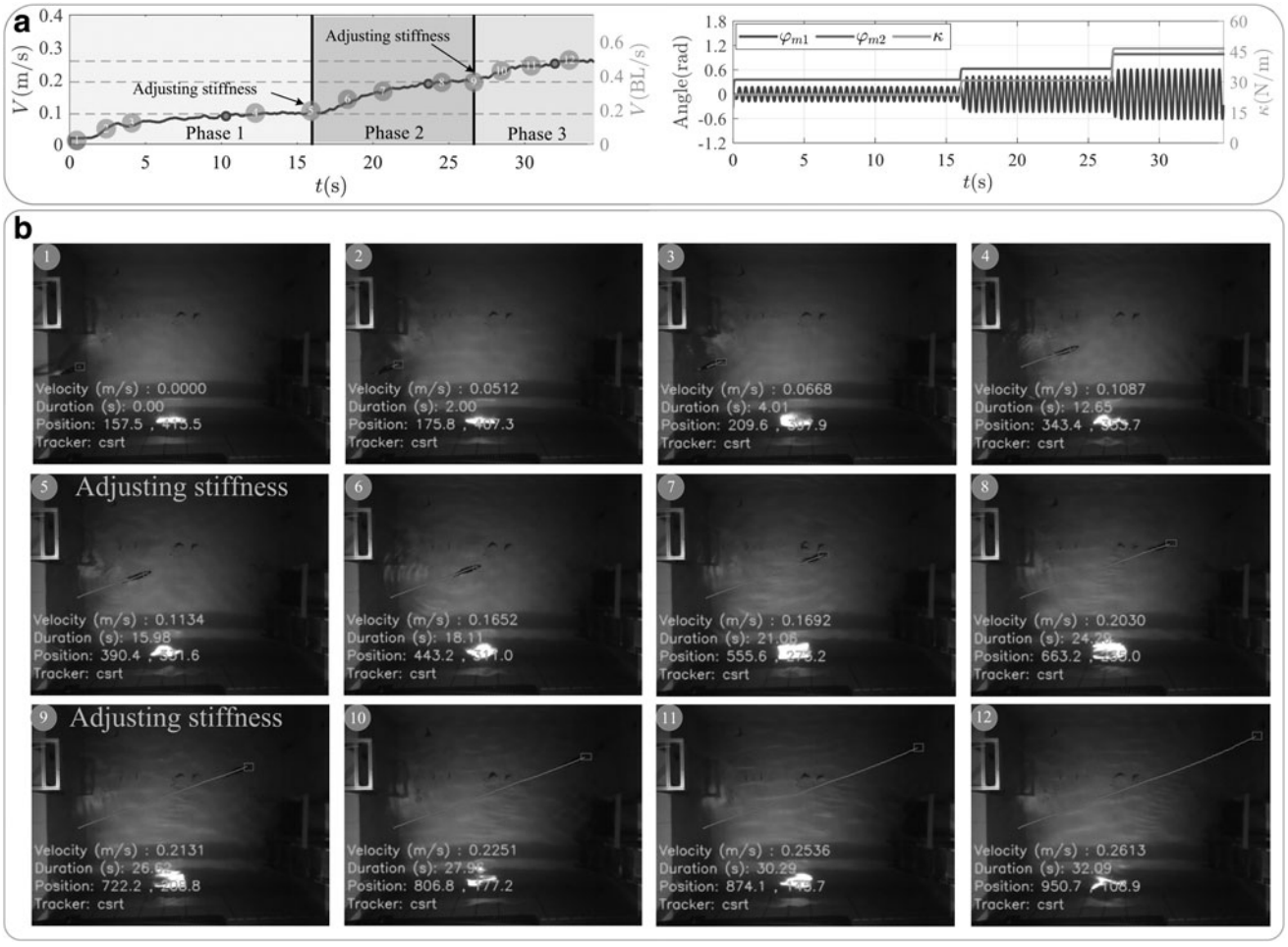

FIG. 8. Experiment of three-stage swimming (See Supplementary Movie S1). **(a)** Experimental data for online variable stiffness swimming. *Left*: Real-time swimming speed of robotic fish. The *dark color dots* indicate that the robotic fish reaches a steady state of swimming. The sequence numbers on the curve correspond with those of snapshots in **(b)**. *Right*: The real-time output angles of the fishtail actuating servomotor and stiffness adjusting servomotor, as well as the real-time stiffness. The swimming process includes three stages. In the first stage, fishtail stiffness is adjusted to 23.75 N/m, and frequency and amplitude are 2.25 Hz and 10°, respectively. Robotic fish begins to accelerate and reaches a stable speed of 0.093 m/s at 10.3 s. At about 15.98 s, fishtail stiffness is adjusted to 30.77 N/m, and frequency and amplitude are adjusted to 2.25 Hz and 25°, respectively. Robotic fish continues to accelerate and achieves a stable speed of 0.192 m/s after 7.67 s. At about 26.62 s, fishtail stiffness is adjusted to 46.5 N/m, and frequency and amplitude are adjusted to 2.25 Hz and 35°, respectively. Robotic fish continues to accelerate and finally reaches a maximum swimming speed of 0.257 m/s after 5.37 s. **(b)** Snapshot sequences of three-stage swimming with real-time stiffness adjustment. In snapshots 5 and 9, robotic fish tunes stiffness based on the optimized stiffness adjustment strategy, to track preset desired speeds and maintain low power losses.

Table 1. Comparison with Other Robotic Fish and Biological Fish

					Adjustable stiffness				
Classification	*Platform*	*Frequency (Hz)*	*Speed (BL/s)*	*COT (J/[m·kg])*	*Adjustable*	*Method*	*Response time (s)*	*Dynamic range*	*Untethered*
Robotic fin	ER-based fin[19]	N/A	N/A	N/A	Yes	Online	N/A	N/A	No
Robotic fish	SMA robotic fish[20]	4	0.64	14.29	Yes	Online	↑: 40 ↓: 10	≈1.56	Yes
Robotic fishtail	Pneumatic fishtail[21]	N/A	N/A	N/A	Yes	Online	N/A	≈1.57	No
Robotic fish	Hydraulic variable stiffness robotic fish[22]	1.25	0.63	N/A	Yes	Online	N/A	≈3.6	Yes
Robotic fishtail	Compress base robotic fishtail[23]	1.2	N/A	N/A	Yes	Online	N/A	≈3.33	No
Underwater robot	Pretension variable stiffness robot[24]	1	N/A	N/A	Yes	Online	N/A	N/A	No
Robotic fish	Pretension robotic fish[25]	6	N/A	N/A	Yes	Online	N/A	N/A	No
Robotic fish	Pretension robotic fish[26]	2.2	1.04	N/A	Yes	Online	N/A	N/A	Yes
Robotic fish	Single-motor-actuated robotic fish[15]	12.82 5	3.8 1.1	94.7 55.5	Yes	Offline	N/A	N/A	Yes
Robotic fish	Flexible-passive-rowing-joint-actuated robotic fish[16]	2	0.3	N/A	Yes	Offline	N/A	N/A	Yes
Robotic fish	Pretension robotic fish[17]	2.4	0.54	N/A	Yes	Offline	N/A	N/A	Yes
Robotic fish	Tunabot[2]	15 5.5	4 1.6	27.8 12.745	No	N/A	N/A	N/A	No
Underwater robot	Reconfigurable armed robot[35]	2	0.2	21	No	N/A	N/A	N/A	Yes
Robotic fish	DEA robotic fish[36]	0.75	0.25	5621	No	N/A	N/A	N/A	Yes
Natural fish	Bluefin tuna[37]	N/A	1.15–1.3	1.23	Yes	Online	Fast	Wide	Yes
Natural fish	Yellowfin tuna[38]	N/A	1.15–1.3	1.1	Yes	Online	Fast	Wide	Yes
Robotic fish	Ours	2.5 1.75	0.81 0.67	8.48 7.14	Yes	Online	↑: 0.26 ↓: 0.26	10.48	Yes

(1) Dynamic range of adjustable stiffness is defined as the ratio of the maximum stiffness to the minimum stiffness; (2) "↑" and "↓" in the column of response time indicate increasing and decreasing stiffness, respectively; (3) "N/A" indicates that the information is not available.

DEA, dielectric elastomer actuators; ER, electrorheological; SMA, shape memory alloy.

a stable swimming state under another stiffness. The settling time is related to the inertia, swimming state (speed, body wave, etc.), fluid, disturbance, and so on. The settling time of swimming for performing two stiffness adjustment in Figure 8 are 7.67 and 5.37 s, respectively. On the other hand, based on the proposed stiffness adjustment strategy, robotic fish can achieve stable and efficient multistage swimming by coordinating the fast and online stiffness adjustment as well as fishtail swing rhythm (e.g., amplitude and frequency), which expands its adaptation in potential applications.

Discussion

Emulating the variable stiffness mechanism of fish in bionics, especially the rapid and large-scale stiffness adjustment, provides an excellent solution for improving the swimming performance of robotic fish.

According to the experimental results, on the one hand, the variable stiffness mechanism designed in this article can achieve a large-scale adjustable stiffness range, and the dynamic range of the adjustable stiffness is about 10.48. A large-scale adjustable stiffness range enables the optimal performance of robotic fish over a wide range of frequencies, such as fast speed and high thrust. On the other hand, the response rate of stiffness adjustment for the designed variable stiffness mechanism is fast, and it can switch to any adjustable stiffness within 0.26 s.

By coordinating the fast and online stiffness adjustment as well as fishtail swing rhythm, robotic fish can achieve stable and efficient swimming, which lays a solid foundation for complex tasks.

In this article, the spring steel, which is not only easy to be manufactured, but also low cost, is used to emulate fish spine. The dimensions of spring steel, such as thickness, width, and length, can be adjusted to achieve different adjustable ranges of fishtail stiffness, which greatly meets the needs of practical applications. In addition, the designed variable stiffness mechanism is installed inside the rigid fish body. When stiffness is adjusted online, the hydrodynamic forces acting on robotic fish do not result in the change of overall shape, and the streamlined shape can be well maintained to improve swimming performance.

Table 1 compares the existing robotic fish, biological fish, and the proposed variable stiffness robotic fish. Although our robotic fish is not superior to the motor-driven robotic fish[2,15] in terms of swimming speed and frequency, it features a lower *COT*. Compared with some robotic fishes,[16,17,20,22,35,36] our robotic fish can obtain a higher swimming speed, and its *COT* is much lower than the former. In addition, the swimming speed and *COT* of our robotic fish are close to those of biological fish, such as bluefin tuna and yellowfin tuna. More importantly, our robotic fish can achieve fast and online stiffness adjustment over a large-scale range, which exists in biological fish to maintain real-time optimal performance.

Conclusions and Future Works

This article proposes a robotic fish that adopts an elastic component to emulate fish spine. It can achieve fast and large-scale stiffness adjustment by tuning the effective length of elastic component. Furthermore, the fishtail stiffness model and Kane-based dynamic model are proposed, the accuracies of both of which are verified by extensive simulations and experiments. The model accuracy provides a solid foundation for analyzing the propulsive performance and motion optimization of robotic fish. Finally, a stiffness adjustment strategy for multistage swimming is constructed. Based on simulations and experiments, the ability of the proposed variable stiffness robotic fish to adjust fishtail stiffness fleetly over a large-scale range in real time is verified.

The focus of future work is placed on the low-power motion control. For example, by optimizing fishtail stiffness and combining stiffness adjustment strategy with motion controllers, we can enable robotic fish to achieve efficient speed or path tracking. Besides, how to optimize the fishtail stiffness of robotic fish to improve maneuverability, for example, low turning radius, and high turning speed, is also a valuable research.

Authors' Contributions

C.Z. designed this study. X.L. performed the simulations and experiments. All authors contributed to the writing and revision of the article, and approved the final article.

Author Disclosure Statement

No competing financial interests exist.

Funding Information

This study was supported by the National Nature Science Foundation of China (62033013, 62003341, and 62203436).

Supplementary Material

Supplementary Appendix SA1
Supplementary Appendix SA2
Supplementary Appendix SA3
Supplementary Appendix SA4
Supplementary Appendix SA5
Supplementary Appendix SA6
Supplementary Appendix SA7
Supplementary Appendix SA8
Supplementary Appendix SA9
Supplementary Appendix SA10
Supplementary Movie S1

References

1. Scaradozzi D, Palmieri G, Costa D, et al. BCF swimming locomotion for autonomous underwater robots: A review and a novel solution to improve control and efficiency. Ocean Eng 2017;130:437–453.
2. Zhu J, White C, Wainwright DK, et al. Tuna robotics: A high-frequency experimental platform exploring the performance space of swimming fishes. Sci Robot 2019;4(34):eaax4615.
3. White CH, Lauder GV, Bart-Smith H. Tunabot Flex: A tuna-inspired robot with body flexibility improves high-performance swimming. Bioinspir Biomim 2021;16(2):026019.
4. Li G, Chen X, Zhou F, et al. Self-powered soft robot in the Mariana Trench. Nature 2021;591(7848):66–71.
5. Aubin CA, Choudhury S, Jerch R, et al. Electrolytic vascular systems for energy-dense robots. Nature 2019; 571(7763):51–57.
6. Marchese AD, Onal CD, Rus D. Autonomous soft robotic fish capable of escape maneuvers using fluidic elastomer actuators. Soft Robot 2014;1(1):75–87.
7. Liu S, Wang Y, Li Z, et al. A fluid-driven soft robotic fish inspired by fish muscle architecture. Bioinspir Biomim 2022;17(2):026009.

8. Zhong Y, Li Z, Du R. A novel robot fish with wire-driven active body and compliant tail. IEEE ASME Trans Mechatron 2017;22(4):1633–1643.
9. Huang C, Lai Z, Zhang L, et al. A magnetically controlled soft miniature robotic fish with a flexible skeleton inspired by zebrafish. Bioinspir Biomim 2021;16(6):065004.
10. Romano D, Wahi A, Miraglia M, et al. Development of a novel underactuated robotic fish with magnetic transmission system. Machines 2022;10(9):755.
11. Chen B, Jiang H. Swimming performance of a tensegrity robotic fish. Soft Robot 2019;6(4):520–531.
12. Park Y-J, Jeong U, Lee J, et al. Kinematic condition for maximizing the thrust of a robotic fish using a compliant caudal fin. IEEE Trans Robot 2012;28(6):1216–1227.
13. Reddy NS, Sen S, Har C. Effect of flexural stiffness distribution of a fin on propulsion performance. Mech Mach Theory 2018;129:218–231.
14. Kancharala AK, Philen MK. Study of flexible fin and compliant joint stiffness on propulsive performance: Theory and experiments. Bioinspir Biomim 2014;9(3):036011.
15. Chen D, Wu Z, Meng Y, et al. Development of a high-speed swimming robot with the capability of fish-like leaping. IEEE ASME Trans Mechatron 2022;27(5):3579–3589.
16. Behbahani SB, Tan X. Design and modeling of flexible passive rowing joint for robotic fish pectoral fins. IEEE Trans Robot 2016;32(5):1119–1132.
17. Li K, Jiang H, Wang S, et al. A soft robotic fish with variable-stiffness decoupled mechanisms. J Bionic Eng 2018;15(4):599–609.
18. Mutlu R, Alici G. Artificial muscles with adjustable stiffness. Smart Mater Struct 2010;19(4):045004.
19. Behbahani SB, Tan X. Design and dynamic modeling of electrorheological fluid-based variable-stiffness fin for robotic fish. Smart Mater Struct 2017;26(8):085014.
20. Liu S, Liu C, Liang Y, et al. Tunable stiffness caudal peduncle leads to higher swimming speed without extra energy. IEEE Robot Autom Lett 2023;8(9):5886–5893.
21. Jusufi A, Vogt DM, Wood RJ, et al. Undulatory swimming performance and body stiffness modulation in a soft robotic fish-inspired physical model. Soft Robot 2017;4(3):202–210.
22. Ju I, Yun D. Hydraulic variable stiffness mechanism for swimming locomotion optimization of soft robotic fish. Ocean Eng 2023;286:115551.
23. Park Y-J, Huh TM, Park D, et al. Design of a variable-stiffness flapping mechanism for maximizing the thrust of a bio-inspired underwater robot. Bioinspir Biomim 2014;9(3):036002.
24. Ziegler M, Hoffmann M, Carbajal JP, et al. Varying Body Stiffness for Aquatic Locomotion. In: 2011 IEEE International Conference on Robotics and Automation IEEE: Shanghai, China; 2011; pp. 2705–2712.
25. Zhong Q, Zhu J, Fish FE, et al. Tunable stiffness enables fast and efficient swimming in fish-like robots. Sci Robot 2021;6(57):eabe4088.
26. Qiu C, Wu Z, Wang J, et al. Locomotion optimization of a tendon-driven robotic fish with variable passive tail fin. IEEE Trans Ind Electron 2022;70(5):4983–4992.
27. Mchenry MJ, Pell CA. Mechanical control of swimming speed: Stiffness and axial wave form in undulating fish models. J Exp Biol 1995;198(11):2293–2305.
28. Matthews DG, Zhu R, Wang J, et al. Role of the caudal peduncle in a fish-inspired robotic model: How changing stiffness and angle of attack affects swimming performance. Bioinspir Biomim 2022;17(6):066017.
29. Long Jr, JH. Muscles, elastic energy, and the dynamics of body stiffness in swimming eels. Am Zool 1998;38(4):771–792.
30. Long Jr, JH, McHenry M, Boetticher N. Undulatory swimming: How traveling waves are produced and modulated in sunfish (Lepomis gibbosus). J Exp Biol 1994;192(1):129–145.
31. Quinn D, Lauder G. Tunable stiffness in fish robotics: mechanisms and advantages. Bioinspir Biomim 2021;17(1):011002.
32. Long Jr, JH, Nipper K S. The importance of body stiffness in undulatory propulsion. Am Zool 1996;36(6):678–694.
33. Tytell ED, Lauder GV. The C-start escape response of Polypterus senegalus: Bilateral muscle activity and variation during stage 1 and 2. J Exp Biol 2002;205(17):2591–2603.
34. Ijspeert AJ, Crespi A, Ryczko D, et al. From swimming to walking with a salamander robot driven by a Spinal Cord Model. Science 2007;315(5817):1416–1420.
35. Paschal T, Shintake J, Mintchev S, et al. Development of Bio-Inspired Underwater Robot with Adaptive Morphology Capable of Multiple Swimming Modes. In: 2017 IEEE/RSJ International Conference on Intelligent Robots and Systems (IROS). IEEE: Vancouver, BC; 2017; pp. 4197–4202.
36. Shintake J, Cacucciolo V, Shea H, et al. Soft biomimetic fish robot made of dielectric elastomer actuators. Soft Robot 2018;5(4):466–474.
37. Blank JM, Farwell CJ, Morrissette JM, et al. Influence of swimming speed on metabolic rates of Juvenile Pacific Bluefin Tuna and Yellowfin Tuna. Physiol Biochem Zool 2007;80(2):167–177.
38. Di Santo V, Kenaley CP, Lauder GV. High postural costs and anaerobic metabolism during swimming support the hypothesis of a U-shaped metabolism–speed curve in fishes. Proc Natl Acad Sci USA 2017;114(49):13048–13053.

Address correspondence to:
Chao Zhou
Laboratory of Cognition and Decision Intelligence for Complex Systems
Institute of Automation
Chinese Academy of Sciences
No. 95 Zhongguancun East Street
Hai-Dian District
Beijing, 100190
China

E-mail: chao.zhou@ia.ac.cn

Long Cheng
State Key Laboratory of Multimodal Artificial Intelligence Systems
Institute of Automation
Chinese Academy of Sciences
No. 95 Zhongguancun East Street
Hai-Dian District
Beijing, 100190
China

E-mail: long.cheng@ia.ac.cn

Junfeng Fan
Laboratory of Cognition and Decision Intelligence for Complex Systems
Institute of Automation
Chinese Academy of Sciences
No. 95 Zhongguancun East Street
Hai-Dian District
Beijing, 100190
China

E-mail: junfeng.fan@ia.ac.cn